The initial ocular following responses elicited by apparent motion stimuli: reversal by inter-stimulus intervals

B. M. Sheliga, **K. J. Chen**, **E. J. FitzGibbon**, and **F. A. Miles**
Laboratory of Sensorimotor Research National Eye Institute National Institutes of Health Bethesda, MD 20892

Abstract

Transient apparent-motion stimuli, consisting of single ¼-wavelength steps applied to square-wave gratings lacking the fundamental ("missing fundamental stimulus") and to sinusoidal gratings, were used to elicit ocular following responses (OFRs) in humans. As previously reported [Sheliga, Chen, FitzGibbon & Miles (2005) Initial ocular following in humans: A response to first-order motion energy. *Vision Research,* In press], the earliest OFRs were strongly dependent on the motion of the major Fourier component, consistent with early spatio-temporal filtering prior to motion detection, as in the well-known energy model of motion analysis. Introducing inter-stimulus intervals (ISIs) of 10–200 ms, during which the screen was gray with the same mean luminance, reversed the initial direction of the OFR, the peak reversed responses (with ISIs of 20–40 ms) being substantially greater than the non-reversed responses (with an ISI of 0 ms). When the mean luminance was reduced to scotopic levels, reversals now occurred only with ISIs≥60 ms and the peak reversed responses (with ISIs of 60–100 ms) were substantially smaller than the non-reversed responses (with an ISI of 0 ms). These findings are consistent with the idea that initial OFRs are mediated by 1st-order motion-energy-sensing mechanisms that receive a visual input whose temporal impulse response function is strongly biphasic in photopic conditions and almost monophasic in scotopic conditions.

Keywords

temporal impulse response; energy-based mechanisms; missing fundamental; scotopic vision

1. Introduction

There is general agreement that there are at least two different mechanisms by which visual motion is sensed: for recent review see Lu & Sperling (2001) and Derrington, Allen & Delicato (2004). On the one hand, there is evidence for a low-level mechanism, which utilizes dedicated local motion sensors that function without regard for form or perceptual features and has been variously referred to as, "short-range", "1st-order", "Fourier-based", "passive", and "energy-based". On the other hand, higher-level mechanisms have been proposed because human observers are able to see moving stimuli that are invisible to these low-level motion sensors— being defined not by luminance but by contrast, disparity or flicker, for example. These higher-level mechanisms have been variously described, in accordance with some attribute of their preferred motion stimulus, as "long-range", "2nd-order", "non-Fourier-based", "active", "feature-based" and "correspondence-based", but it is still not clear if these are all sensed by one or several (different) mechanisms. In this paper we will be concerned with the temporal dynamics of the visual inputs to the motion detectors mediating the initial ocular following responses (OFRs), which are the machine-like tracking eye movements that can be elicited at

Address correspondence to: B. M. Sheliga, Laboratory of Sensorimotor Research, National Institutes of Health Building 49 Room 2A50 49 Convent Drive Bethesda MD 20892-4435 USA Tel: 301-402-4962 FAX: 301-402-0511 email: bms@lsr.nei.nih.gov.

ultra-short latency by sudden motion of a large textured pattern (Gellman, Carl & Miles, 1990; Miles, Kawano & Optican, 1986). Recent findings suggest that the initial OFRs are mediated by the low-level mechanism which utilizes motion detectors that are sensitive to 1st-order motion energy, as in the well-known energy model of motion analysis (Adelson & Bergen, 1985; van Santen & Sperling, 1985; Watson & Ahumada, 1985). Accordingly, OFRs show clear reversal with "1st-order reverse-phi motion", one of the hallmarks of an energy-based mechanism (Masson, Yang & Miles, 2002a), and are very sensitive to the Fourier composition of the luminance modulations in the motion stimulus (Chen, Sheliga, Fitzgibbon & Miles, 2005; Sheliga, Chen, FitzGibbon & Miles, 2005). The visual stimuli in these most recent studies included vertical square-wave gratings lacking the fundamental—referred to as the missing fundamental (*mf*) stimulus—and motion was applied in successive ¼-wavelength steps. The initial OFRs associated with this motion stimulus were always reversed, i.e., rightward steps resulted in leftward OFRs. In fact, it had been known for some time that the perceived direction of motion was often reversed when ¼-wavelength steps were applied to the *mf* stimulus (Adelson, 1982; Adelson & Bergen, 1985; Baro & Levinson, 1988; Brown & He, 2000; Georgeson & Harris, 1990; Georgeson & Shackleton, 1989). The explanation advanced for this apparent reversal of initial OFRs and perceived motion is that the underlying detectors do not sense the motion of the raw images (or their features) but rather a spatially filtered version of the images, so that the perceived motion depends critically on the Fourier composition of the spatial stimulus. In the frequency domain, a pure square wave is composed entirely of the odd harmonics (1st, 3rd, 5th, 7th etc.,) with progressively decreasing amplitudes such that the amplitude of the *i*th harmonic is proportional to $1/i$. Accordingly, the *mf* stimulus lacks the 1st harmonic and so is composed entirely of the higher odd harmonics, with the 3rd having the lowest spatial frequency and the largest amplitude. This means that when the *mf* stimulus shifts ¼ of its (fundamental) wavelength, the largest Fourier component, the 3rd harmonic, shifts ¾ of its wavelength in the same (forward) direction. However, a ¾-wavelength *forward* shift of a sine wave is exactly equivalent to a ¼-wavelength *backward* shift and, because the brain gives greatest weight to the nearest image matches (spatial aliasing), the OFR and the perceived motion are in the *backward* direction. In fact, when ¼-wavelength steps are applied to the *mf* stimulus, all of the 4*n*-1 harmonics (where *n* is an integer), such as the 3rd, 7th, 11th etc., will shift ¼ of their wavelength in the *back*ward direction and all of the 4*n*+1 harmonics, such as the 5th, 9th, 13th etc., will shift ¼ of their wavelength in the *for*ward direction. Of course, each of the harmonics has a different apparent speed because the higher the spatial frequency the smaller the absolute magnitude of the (¼-wavelength) shifts.

Georgeson and Harris (1990) studied the perceived motion associated with ¼-wavelength steps applied to *mf* gratings and examined the effect of introducing blank inter-stimulus intervals (ISIs) of 5–320 ms between each of the steps. With the shorter ISIs (20 ms or less), the perceived motion was still in the backward direction of the 3rd harmonic, but with the longer ISIs (40 ms or more) the perceived motion was often reversed, i.e., in the forward direction of the pattern or feature. These workers suggested that motion perception results from a 1st-order energy-based mechanism with the shorter ISIs and from the displacement of features with the longer ISIs, consistent with the idea that the feature-based mechanism has the longer time constant and so can integrate motion over much longer time periods than the energy-based mechanism, which is effectively disabled by the longer ISIs (cf., Braddick, 1980). A number of other authors have also advanced this same (or a very similar) explanation for the reversal of perceived motion by an ISI (Bex & Baker, 1999; Boulton & Baker, 1993; Brown & He, 2000; Derrington et al., 2004; Hammett, Ledgeway & Smith, 1993; Smith, 1994). However, others (Pantle & Turano, 1992; Shioiri & Cavanagh, 1990; Strout, Pantle & Mills, 1994; Takeuchi & De Valois, 1997; Takeuchi, De Valois & Motoyoshi, 2001) have reported reversals of perceived motion with ISIs less than ~100 ms that they attributed to the temporal dynamics of the early visual pathway, invoking the negative phase of the well-known biphasic temporal impulse response function of the human visual system, often inferred from the band-pass temporal dynamics

observed with sinusoidal flicker (Bergen & Wilson, 1985; Burr & Morrone, 1996; Ikeda, 1965; 1986; Kelly, 1961; 1971a; 1971b; Rashbass, 1970; Roufs, 1972a; 1972b; Swanson, Ueno, Smith & Pokorny, 1987). [1] Importantly, some of the reports that invoked this temporal-dynamics explanation used sine-wave stimuli for which the motion energy and features always move in the same direction, hence ruling out the possibility (in these cases, at least) that the ISI-induced reversal reflected a transition from a 1st-order energy-based mechanism to a feature-based one (Strout et al., 1994; Takeuchi & De Valois, 1997; Takeuchi et al., 2001). A critical feature of this temporal-dynamics hypothesis is that the neural representation of the images in the visual pathways leading to the underlying motion detectors undergoes transient reversal (duration, less than ~100 ms) during the ISIs. The study of Takeuchi & De Valois (1997) used sine-wave gratings with a wide range of ISIs and reported reversal of perceived motion with intermediate ISIs (30–90 ms) but a return to veridical (i.e., correct) motion with long ISIs (105–500 ms). These workers suggested that 1st-order mechanisms with brisk dynamics and a short time constant mediate the perceived motion with short and intermediate ISIs (less than ~100 ms)—the reversals during this time resulting from the temporal dynamics of the early visual pathway—whereas feature-based mechanisms with more sluggish dynamics and a longer time constant mediate the veridical motion perceived with long ISIs (more than ~100 ms). This opens up the possibility that the ISI-induced reversals of perceived motion in the earlier study of Georgeson and Harris (1990) using *mf* stimuli might have resulted from the temporal dynamics of the 1st-order motion-energy mechanism with intermediate ISIs (less than ~100 ms?) and from the feature-based mechanism only with longer ISIs. Takeuchi & De Valois (1997) also showed that reducing the contrast to 3-times threshold eliminated the perceived motion associated with long ISIs but not that with short/intermediate ISIs, consistent with the suggestion that feature-based mechanisms have lower contrast sensitivity than 1st-order energy-based mechanisms (Lu & Sperling, 1995; Nishida, 1993; Smith, Hess & Baker, 1994; Solomon & Sperling, 1994). Furthermore, they showed that the reversal at intermediate ISI (30–90 ms) does not occur at scotopic luminance levels (0.0785 photopic td), consistent with the known shift from band-pass to low-pass temporal characteristics in the frequency domain (and so from a biphasic to a monophasic transient response in the time domain) as adapting luminance levels are decreased (Kelly, 1971a; 1971b; Roufs, 1972a; 1972b; Snowden, Hess & Waugh, 1995; Swanson et al., 1987). Others have also provided evidence in support of the idea that perceived motion results from 1st-order motion energy mechanisms at short/intermediate ISI and feature-based mechanisms at long ISI using motion stimuli consisting of Gabor patches (Bex & Baker, 1999) and gratings composed of two different sinusoids (Hammett et al., 1993).

Here we report in Experiment 1 that the initial OFRs elicited by ¼-wavelength steps applied to *mf* and pure sine-wave stimuli at photopic luminance levels are reversed by ISIs of 10–200 ms, the peak reversed responses (with ISIs of 20–40 ms) being substantially greater than the usual non-reversed responses (with an ISI of 0 ms). In Experiment 2 we show that this reversal with ISIs was evident even at very low contrasts. Lastly, in Experiment 3 we show that at scotopic luminance levels, reversals occurred only with ISI≥60 ms and even the largest reversed responses (with ISIs of 60–100 ms) were always substantially smaller in amplitude than the non-reversed responses (with an ISI of 0 ms). These findings are consistent with the idea that initial OFRs are mediated by 1st-order motion-energy-sensing mechanisms that receive a visual input whose temporal impulse response is strongly biphasic in photopic conditions and almost monophasic in scotopic conditions. Some aspects of Experiment 1 have been published in a preliminary form (Chen et al., 2005).

---

[1]The reversal of perceived motion by an ISI was first reported by Braddick (1980), who offered no explanation.

2. Experiment 1: Dependence of the initial OFR on the duration of an ISI

This first experiment concentrated on the effects of ISIs on the initial OFR to *mf* and sine-wave apparent-motion stimuli under photopic conditions.

2.1. Methods

Some of the techniques, such as those used for recording eye movements and for data analysis, were very similar to those used previously in our laboratory (Masson, Busettini, Yang & Miles, 2001; Masson, Yang & Miles, 2002b; Sheliga et al., 2005; Yang & Miles, 2003) and, therefore, will only be described in brief here. Experimental protocols were approved by the Institutional Review Committee concerned with the use of human subjects.

2.1.1. Subjects—Three subjects participated; two were authors (KJC, FAM) and the third was a paid volunteer who was unaware of the purpose of the experiments (JKM). Viewing was binocular for KJC and FAM, and monocular for JKM (right eye viewing). All had normal or corrected-to-normal vision.

2.1.2. Visual display and the grating stimuli—The subjects sat in a dark room with their heads positioned by means of adjustable rests for the forehead and chin and held in place with a head band. Visual stimuli were presented on a computer monitor (Silicon Graphics CPD G520K 19" CRT driven by a PC Radeon 9800 Pro video card) located straight ahead at 45.7 cm from the corneal vertex. The monitor screen was 385 mm wide and 241 mm high, with a resolution of 1920 x 1200 pixels and a vertical refresh rate of 100 Hz. The RGB signals from the video card provided the inputs to an attenuator (Pelli & Zhang, 1991) whose output was connected to the "green" input of a video signal splitter (Black Box Corp., AC085A-R2); the three "green" video outputs of the splitter were then connected to the RGB inputs of the monitor. This arrangement allowed the presentation of black and white images with 11-bit grayscale resolution. Initially, a luminance look-up table with 64 equally-spaced luminance levels ranging from 0.5 cd/m^2 to 84.7 cd/m^2 was created by direct luminance measurements (IL1700 photometer; International Light Inc., Newburyport, MA) under software control. This table was then expanded to 2048 equally-spaced levels by interpolation and subsequently checked for linearity (typically, r>0.99996).

Motion stimuli consisted of a two-image movie with an intervening period of gray, the ISI. The two visual images consisted of one-dimensional vertical grating patterns that could have one of three horizontal luminance profiles in any given trial: 1) a sine wave with a spatial frequency of 0.153 cycles/° (wavelength, 6.55°, which was 264 pixels), termed "the *1f* stimulus", 2) a sine wave with a spatial frequency of 0.458 cycles/° (wavelength, 2.183°, which was 88 pixels), termed "the *3f* stimulus", 3) a square wave with a missing fundamental, termed "the *mf* stimulus", with a spatial frequency of 0.153 cycles/°. Note that our previous study (Sheliga et al., 2005) had indicated that the dependence of OFR on log spatial frequency was well represented by a Gaussian function peaking on average at 0.25 cycles/°. The spatial frequencies of the *1f* and *3f* stimuli were chosen to be at symmetrical locations on either side of the peak of the normalized average Gaussian so that the two stimuli had roughly equal efficacy and elicited OFRs whose magnitude was, on average, 89% of that elicited by the peak spatial frequency (0.25 cycles/°). Each image extended 257 mm horizontally (31.4°; 1280 pixels) and 206 mm vertically (25.4°; 1024 pixels) and had a mean luminance of 42.6 cd/m^2. This image was surrounded by a uniform gray border (with this same luminance) that extended out to the boundaries of the screen. The initial phase of the first image was randomized from trial to trial at intervals of ¼-wavelength, and the second image was identical to the first except phase shifted horizontally (rightward or leftward, randomly selected) by 1.65° (66 pixels), corresponding to ¼ of the wavelength of the fundamental of the *1f* and *mf* stimuli and ¾ of the

wavelength of the *3f* stimulus. The Michelson contrast, defined as $((L_{max}-L_{min})/(L_{max}+L_{min}))*100\%$, where L is the luminance, was 32% for the pure sinusoids and for the *3f* component of the *mf* stimulus. The mean (space-averaged) luminance was always 42.6 cd/m^2 throughout the experiment, including the ISI. The dependent variable in this first experiment was the duration of the ISI, randomly sampled each trial from a lookup table specifying the duration in terms of the number of frames: 0, 1, 2, 3, 4, 6, 10, 14, 20 (each frame lasting 10 ms because of the 100 Hz frame rate).

The display had a resolution of 40 pixels/º at the center, so that any components of the *mf* stimuli with spatial frequencies above 20 cycles/º (the Nyquist Frequency) would be aliased to lower frequencies. However, we think that spatial aliasing was not a problem with our *mf* stimuli because the highest contrast of any harmonic above the Nyquist Frequency—the 133rd with a spatial frequency of 20.3 cycles/º—was only 0.9%, which our previous study indicated was very close to the threshold for eliciting OFRs (Sheliga et al., 2005); see also Fig. 4 in the present paper. Note that all spatial frequencies given in this paper refer to the minimum seen value, which is the value at that point on the screen directly ahead of each eye and, because the images were on a tangent screen, the spatial frequency seen by the subject increased with eccentricity from those points.

We shall refer to OFRs that were in the direction of the 1.65º shift as in the *forward* direction, and OFRs in the opposite direction as in the *backward* direction. With the *mf* stimuli, the motion of the features and of the 4n+1 harmonics (of which the most prominent was the 5th) was in the forward direction, whereas the motion of the 4n-1 harmonics (of which the most prominent was the 3rd) was in the backward direction.

2.1.3. Eye-movement recording—The horizontal and vertical positions of the right eye were recorded with an electromagnetic induction technique (Robinson, 1963) using a scleral search coil embedded in a silastin ring (Collewijn, Van Der Mark & Jansen, 1975), as described by Yang, FitzGibbon and Miles (2003).

2.1.4. Procedures—All aspects of the experimental paradigms were controlled by two PCs, which communicated via Ethernet using the TCP/IP protocol. One of the PCs was running a Real-time EXperimentation software package (REX) developed by Hays, Richmond and Optican (1982), and provided the overall control of the experimental protocol as well as acquiring, displaying, and storing the eye-movement data. The other PC was running Matlab subroutines, utilizing the Psychophysics Toolbox extensions (Brainard, 1997; Pelli, 1997), and generated the visual stimuli upon receiving a start signal from the REX machine.

At the beginning of each trial, the first image appeared (randomly selected from a lookup table) together with a central target spot (diameter, 0.25º) that the subject was instructed to fixate. After the subject's right eye had been positioned within 2º of the fixation target for a randomized period of 600 to 900 ms the first image disappeared and the screen changed to a uniform gray with the same mean luminance for $n*10$ ms, where *n* was the number of frames listed in the lookup table for the ISI in that trial. At the end of the ISI, the fixation target was removed and the second image appeared for 20 frames (200 ms). The screen then changed to a uniform gray with the same mean luminance, marking the end of the trial. After an inter-trial interval of 500 ms a new first image appeared together with a fixation target, commencing a new trial. The subjects were asked to refrain from blinking or making any saccades except during the inter-trial intervals but were given no instructions relating to the motion stimuli. If no saccades were detected during the period of the trial (using an eye velocity threshold of 12º/s), then the data were stored on a hard disk; otherwise, the trial was aborted and subsequently repeated. Data were collected over several sessions until each condition had been repeated an adequate number of times to permit good resolution of the responses (through averaging). The actual numbers

of trials per condition will be given in the Results. There were 54 different stimulus conditions (9 ISIs, 3 types of grating pattern, 2 directions of motion).

2.1.5. Data analysis—The horizontal and vertical eye position data obtained during the calibration procedure were each fitted with second-order polynomials which were then used to linearize the horizontal and vertical eye position data recorded during the experiment proper. The eye-position data were first smoothed with a 6-pole Butterworth filter (3 dB at 45 Hz) and then mean temporal profiles were computed for each subject for all the data obtained for each of the stimulus conditions. Because the OFRs elicited by two-image motion stimuli ("velocity impulse responses") were often very weak, the OFRs to rightward and leftward were pooled to improve the signal-to-noise by subtracting the mean response to each leftward motion stimulus from the mean response to the corresponding rightward motion stimulus: the "R-L position responses". As rightward eye movements were positive in our sign convention, these pooled measures were positive when OFRs were in the forward direction. Velocity responses (termed "mean R-L velocity response profiles") were estimated at successive 1-ms intervals by computing the differences between the R-L position responses at intervals of 10 ms. Trials with saccadic intrusions (that had failed to reach the eye-velocity threshold of 12°/s used during the experiment) were deleted. The initial horizontal OFRs were quantified by measuring the amplitude of the initial peak in the mean R-L velocity response profiles (termed "mean R-L peak velocity responses") using the following search algorithm: On a first pass, we measured the first peak whose latency exceeded 70 ms and whose amplitude exceeded 3 times the standard deviation (SD) of the noise during the pre-response period (based on the 40-ms period starting with the onset of the motion stimulus). This provided response measures for all but two responses (2/81) and for these we made a second pass, this time selecting the first peaks (whose latency exceeded 70 ms) by hand. In the figures, response measures that met the 3SD criterion are plotted as black symbols and the two that required hand selection are plotted as gray symbols.

2.2. Results

The initial OFRs elicited by two-image movies with a 0-ms ISI were generally transient and very small: peak velocities were at most a few tenths of a degree per second, as previously reported by Masson et al. (2002a), and were also in accord with our previous findings using more prolonged stimuli insofar as minimum latencies were ~65 ms and the initial responses to the *1f* stimulus were always in the *forward* direction whereas the initial responses when the same shifts were applied to the *mf* and *3f* stimuli were invariably in the *backward* direction (Chen et al., 2005; Sheliga et al., 2005). These features can be seen in Fig. 1, which shows the initial peak in the mean R-L velocity response profiles obtained from one subject with each of the three types of gratings: see the traces labeled "0" (indicating 0-ms ISI) and note that upward deflections of the traces denote forward OFRs. Interposing an ISI lasting 1 or more frames (each frame having a duration of 10 ms) resulted in a clear reversal of the direction of the initial OFRs in all cases: see the traces labeled "10", 20", "40", and "200" (indicating the ISI in ms) in Fig. 1. The latency of the reversed responses was consistently longer than the latency of the non-reversed responses when the ISI was <40 ms. Significantly, the reversed OFRs could reach velocities that were much higher than those reached by the non-reversed OFRs (with 0-ms ISI).

These trends are evident from the quantitative measures plotted in Fig. 2, which shows the dependence of the mean R-L peak velocity responses (upper plots) and the latency of those peaks (lower plots) on the duration of the ISI for all three types of grating patterns and for all three subjects (forward OFRs are positive and plotted upward). The upper plots in Fig. 2 indicate that the reversal of the initial OFR was always evident with the 10-ms ISI and reached a peak as the ISI increased to 20–40 ms, declining thereafter until finally reaching an asymptote as the ISI increased to 100–140 ms. This asymptote invariably fell short of zero (especially in

subject FAM), though sometimes approaching very close (*3f* and *mf* data for subject KJC; *1f* and *mf* data for subject JKM). As in our previous study (Sheliga et al., 2005), the OFRs obtained with the *mf* stimuli were generally weaker than those obtained with the *3f* stimuli (whose contrast matched that of the 3rd harmonic of the *mf* stimulus). The reversed OFRs reached peak velocities that exceeded those reached by the non-reversed OFRs, on average by 553% (range, 84–2152%). The lower plots in Fig. 2 indicate that the increase in latency that accompanied response reversal (as evidenced by the latency of the peak velocity) was generally greatest for the 10-ms ISI and declined rapidly with longer ISI.

2.3. Discussion of Experiment 1

Inter-stimulus intervals of 10–60 ms induced clear reversal of the initial OFRs with all three stimuli (*1f*, *3f*, *mf*), and this reversal sometimes persisted, albeit weakly, with the longest ISI that we used (200 ms). The ISI-induced reversals of the OFR to pure sinusoidal stimuli could not have been due to a feature-based mechanism, lending further support to our recent study which strongly suggested that the initial OFR is driven exclusively by 1st-order motion energy (Sheliga et al., 2005). Our new findings are reminiscent of the many previous reports that described reversals of perceived motion by ISIs (Bex & Baker, 1999; Boulton & Baker, 1993; Georgeson & Harris, 1990; Pantle & Turano, 1992; Shioiri & Cavanagh, 1990; Strout et al., 1994; Takeuchi & De Valois, 1997; Takeuchi et al., 2001). As indicated in the Introduction (Section 1), the general suggestion from these earlier studies is that with ISIs of less than ~100 ms the perceived motion depends on 1st-order energy-based mechanisms, whereas with longer ISIs the perceived motion depends on higher-order feature-based mechanisms. That the ISI-induced reversal of the OFR in our present study occurred with short/ intermediate ISIs is again consistent with their mediation by 1st-order motion energy. Most authors attribute the ISI-induced reversal of perceived motion to the temporal dynamics of the visual input reaching the motion detectors, i.e., the negative phase of the biphasic temporal impulse response, and we think that this is also responsible for the ISI-induced reversal of the OFR in the present paper. In this scheme, the polarity of the visual responses reaching the underlying motion detectors is assumed to undergo reversal during the ISI. Thus, the neural representation of the 2nd image—whose appearance marks the onset of motion in our experiments—is matched to a representation of the 1st image that is assumed to have one polarity when there is no ISI and the reverse polarity when there is an ISI of <100 ms. This is equivalent to a 180º phase shift so that the ¼-wavelength difference between our 1st and 2nd images would be seen as a 90º phase shift in one direction when there was no ISI and a 90º phase shift in the reverse direction when there was an ISI of <100 ms.

The effects of ISIs on the OFRs obtained with the *mf* stimuli were very similar to the effects of ISIs on the OFRs obtained with the *3f* stimuli except for being somewhat weaker, in line with our previous findings which indicated that the OFRs to the *mf* stimuli are largely due to the principal Fourier component, the 3rd harmonic, but that there is often a significant contribution from the 5th (and higher?) harmonics (Sheliga et al., 2005). In their landmark study using *mf* stimuli, Georgeson and Harris (1990) reported reversals of perceived motion with ISIs of 40–320 ms and attributed them entirely to a feature-based mechanism. Our study suggests that this might not have been the case for the reversals seen with the shorter ISIs (see also Takeuchi & De Valois, 1997).

Small reversed OFRs were still present in our experiments even when the ISI was >100 ms, implying a minor contribution from an energy–based mechanism with a somewhat longer time constant than that generally found in psychophysical experiments on perceived motion. It might be argued that such a contribution could have obscured feature-based responses with longer ISIs in our study. This was one of the reasons why we next examined the effect of ISIs when

the motion stimuli had low contrast, cf., Georgeson & Harris (1990) and Takeuchi & De Valois (1997).

Tong, Wang & Sun (2002) recorded the closed-loop optokinetic nystagmus (OKN) evoked by sine-wave gratings undergoing successive ¼-wavelength shifts with ISIs ranging from 17 to 100 ms. These workers reported that with the shortest ISI (17 ms) the slow-phase eye velocity was always in the normal (forward) direction, but with the longer ISIs the slow phases alternated periodically between the forward and the reverse direction, each alternation lasting several seconds in the data shown. These workers linked this response pattern to "the alternation of perceived motion" and invoked the biphasic temporal impulse response to explain the periods of reversal. The problem with the closed-loop situation used here is that the movement of the eyes would disrupt the orderly presentation of the (intermittent) stimulus on the retina. For the data shown in their Fig. 2, for instance, we estimate that the slow-phase eye speed often exceeded 10º/s, so that the eyes would undergo appreciable movement during each ISI. When the ISI was 50 ms, for example, the eye movement during the blank periods would often exceed ¼ of the wavelength of the grating that was used (0.5cycles/º). In addition there were many quick phases that would also affect the phase of the gratings on the retina. In sum, the combination of, 1) a periodic visual stimulus, 2) intermittent exposure to the motion stimulus, and 3) eye movements (quick-phases as well as slow-phases), create a serious spatial aliasing problem, rendering the exact etiology of the associated eye movements uncertain. In a subsequent paper it was reported that a similar pattern of alternating eye movements was observed even when the grating pattern was stationary (Tong, Peng & Sun, 2003). The lack of control of the sequence of images on the retina severely limits the utility of these closed-loop approaches and it was to avoid such uncertainty that we restricted our studies to the initial open-loop OFRs elicited by two-image movies.

3. Experiment 2: Reversal of the OFR by ISIs and its dependence on contrast

Takeuchi & De Valois (1997), using sine-wave gratings, showed that when the contrast was reduced to only 3-times threshold the perceived motion with short/intermediate ISIs was preserved (i.e., veridical with ISI<30 ms, reversed with ISI of 30–90 ms) whereas the normally veridical perceived motion with long ISIs (>100 ms) was completely eliminated. This was consistent with the idea that, 1) perceived motion is mediated by 1st-order energy-based mechanisms at short/intermediate ISIs and by feature-based mechanisms at long ISIs, and 2) the 1st-order mechanisms have the higher contrast sensitivity (Lu & Sperling, 1995; Nishida, 1993; Smith et al., 1994; Solomon & Sperling, 1994). In broad agreement with this, the experiments of Georgeson & Harris (1990), using the *mf* stimulus, demonstrated that at moderately low contrast (4%) and short exposures to the gratings (30 ms) the usual perceived motion with short ISI (<40 ms), which was in the direction of the 3rd harmonic (i.e., reversed) was preserved but the usual perceived motion with longer ISIs (>40 ms), which was in the direction of the features (i.e., veridical), was eliminated. We now report findings from two experiments using sine-wave gratings in which we examined the effects of ISIs on initial OFRs at different contrasts. The data from Experiment 2A indicate that the general dependency of OFRs on ISIs seen with high-contrast patterns (32%) in Experiment 1 is still evident at lower contrasts (12%, 4%), consistent with mediation by mechanisms sensitive to 1st-order motion energy. The data from Experiment 2B indicate that the reversed OFRs recorded with a 40-ms ISI generally show a very similar dependency on contrast to the non-reversed OFR recorded with 0-ms ISI, consistent with mediation by the same neural elements and sensing mechanism.

3.1. Methods

Most of the methods and procedures were identical to those used in Experiment 1, and only those that were different will be described here.

3.1.1. Subjects—Three subjects participated in both experiments: two were authors (KJC and FAM in Experiment 2A; BMS and FAM in Experiment 2B) and the third was a paid volunteer who was unaware of the purpose of the experiments (JKM in Experiment 2A and NPB in Experiment 2B).

3.1.2. Grating patterns—Motion stimuli again consisted of a two-image movie, this time using only pure sine-wave gratings of spatial frequency 0.458 cycles/° (wavelength, 2.183°, which was 88 pixels). This was the same as the "*3f* stimulus" used in Experiment 1. The initial phase of the first image was randomized from trial to trial at intervals of ¼-wavelength, and the second image was identical to the first except phase shifted horizontally (rightward or leftward, randomly selected) by 1.65° (66 pixels), corresponding to ¾ of the wavelength of the *3f* stimulus, exactly as in Experiment 1. This means that the signs of the responses were the same in Experiments 1 and 2, facilitating direct comparisons. In Experiment 2A, the ISIs were 0, 10, 20, 40, 60, 100, 140, and 200 ms, and gratings could have one of three Michelson contrasts: 4%, 12% and 36%. In Experiment 2B, the ISIs were 0 and 40 ms, and the gratings could have one of 8 contrasts: 0.5%, 1%, 2%, 4%, 8%, 16%, 32%, and 64%.

3.1.3. Procedures—These were as in Experiment 1 except that each block of trials had 48 randomly interleaved stimulus combinations in Experiment 2A (3 contrasts, 8 ISIs, 2 directions of motion) and 32 such stimulus combinations in Experiment 2B (8 contrasts, 2 ISIs, 2 directions of motion).

3.2. Results

The data obtained in Experiment 2A are plotted in Fig. 3, which shows the dependence on ISI of the mean R-L peak velocity response (upper plots) and of the latency of those peaks (lower plots) for gratings of three contrasts for each of the three subjects, cf., Fig. 2. The data obtained with the highest contrast (36%: open circles) were essentially the same as those obtained with the *3f* stimuli in Experiment 1, which were of similar contrast (32%): again, there were clear response reversals that peaked with ISIs of 20–40 ms and declined to a non-zero asymptote as ISIs reached ~100 ms, and peak latencies increased with the shorter ISIs (10–30 ms). The peak responses achieved with the lower contrast stimuli (12%, 4%) were often weaker than those achieved with the higher contrast stimuli (36%)—especially with ISIs<100 ms—but otherwise showed a very similar general dependence on the ISI. Peak responses of 2/3 subjects (JKM, KJC) showed little dependence on contrast with ISIs≥100 ms. The latency of the peaks was generally longer with the lower contrast stimuli, especially with ISIs of 60 ms or more. Note that only 1/72 responses failed to reach the 3SD criterion and was selected by hand (gray symbols in Fig. 3C,F).

The data obtained in Experiment 2B are plotted in Fig. 4, which shows the contrast dependence (plotted on a log abscissa) of the mean R-L peak velocity responses (upper plots) and of the latency of those peaks (lower plots) when ISIs were 0 ms (open circles) and 40 ms (closed circles) for each of the three subjects. Note that when the contrast was <2%, 10/12 response measures failed to reach the 3SD criterion and so in these cases, as in the earlier experiments, we simply selected the first peak whose latency exceeded 70 ms (by hand) and these data are plotted in gray in Fig. 4. Most peak responses show a monotonic rise from a threshold and were fitted with the following expression:

$$R_{max}\frac{c^n}{c^n + c_{50}^n};$$

(1)

where R_{max} is the maximum attainable response, c is the contrast, c_{50} is the semi-saturation contrast (at which the response has half its maximum value), and n is the exponent that sets the steepness of the curves. This expression is based on the Naka-Rushton equation (Naka &

Rushton, 1966), and our recent study (Sheliga et al., 2005), together with that of Masson & Castet (2002), indicated that it generally provides a good fit to the contrast dependence curves for the initial OFR in humans. The continuous smooth lines in the upper plots in Fig. 4 are the best-fit curves using Expression 1 and, given that r^2 values were >0.94 in all cases, these clearly provide a reasonably good description of the data. The parameters, c_{50} and n, for these various fits are printed beside the curves in Fig. 4 and indicate that the dependence on contrast was very similar for the 0-ms and the 40-ms data. Thus, values for the n parameter ranged only from 2.40 to 4.28 and differed by only 1.61, 0.58 and 0.62 for the three subjects. Values for the c_{50} parameter ranged only from 1.9% to 3.9% and, although the 40-ms data consistently exceeded those for the 0-ms data the difference was quite small: 1.0%, 0.8% and 0.1% in the 3 subjects.[2] The latencies of the initial response peaks (lower plots in Fig. 4) showed a steady rise as contrast was decreased from 64% to 2%, though for any given contrast, the latencies for the 40-ms data (closed circles) generally exceeded those for the 0-ms data (open circles) slightly: mean differences were 1.3 ms, 3.7 ms, and 1.3 ms, for the 3 subjects.

3.3. Discussion of Experiment 2

The effects of ISIs on the initial OFR were relatively independent of contrast. The clear reversals of the OFR by ISIs<100 ms that were seen in Experiment 1 with high-contrast gratings (32%) were still evident in Experiment 2 with contrasts as low as 2% (Fig. 4). Further, although the initial OFRs were often much weaker with the lower-contrast stimuli, it was clear from Fig. 3 that the general form of their dependence on the ISI was very similar for all three contrasts used (4%, 12%, 36%). These findings are consistent with the suggestion that initial OFRs are mediated by 1st-order motion-energy detectors, which are generally thought to be more sensitive to low contrast than are feature-based mechanisms (Lu & Sperling, 1995;Nishida, 1993;Smith et al., 1994;Solomon & Sperling, 1994;Takeuchi & De Valois, 1997). That the dependence of the reversed OFRs on contrast when the ISI was 40 ms was very similar to the dependence of the non-reversed OFRs on contrast when the ISI was 0 ms—based on the similarity of the best-fit parameters of the Naka-Rushton equation—is consistent with their mediation by the same visual pathways and motion sensors in accordance with the proposition that the reversals result solely from the temporal dynamics of those visual pathways.

The small reversed OFRs seen in Experiment 1 with high-contrast gratings when ISIs exceeded 100 ms were still evident with the lowest contrast used in Experiment 2A—4% (Fig. 3)— further reinforcing the idea that they are mediated by a 1st-order energy-based sensing mechanism as proposed earlier in Section 2.3 (Discussion of Experiment 1).

4. Experiment 3: Effects of ISIs on the initial OFR at scotopic luminance levels

Experiments 1 and 2 showed that ISIs resulted in clear reversal of the initial OFR and we argued that this was consistent with numerous psychophysical studies, which had indicated that the human visual system had band-pass characteristics in the frequency domain and biphasic transient characteristics in the time domain (Bergen & Wilson, 1985; Burr & Morrone, 1996; Ikeda, 1965; 1986; Kelly, 1961; 1971a; 1971b; Rashbass, 1970; Roufs, 1972a; 1972b; Snowden et al., 1995; Spekreijse, van Norren & van den Berg, 1971; Swanson et al., 1987). However, this describes the situation under photopic viewing conditions and it is known that under scotopic viewing conditions the system has frequency characteristics that are much more low-pass and, correspondingly, temporal characteristics that are much more monophasic (Kelly, 1961; 1971a; 1971b; Roufs, 1972a; 1972b; Snowden et al., 1995; Swanson et al., 1987). The reversal of perceived motion with intermediate ISIs (30-90 ms) reported by Takeuchi & De

---

[2]These estimates of c_{50} and n were obtained from fits that used all of the response measures plotted in Fig. 4 A-C, including those that failed to reach the 3SD criterion (plotted in gray). Forcing the measures plotted in gray to zero had negligible effects on the parameters.

Valois (1997) was obtained under photopic viewing conditions and these workers also showed that the reversal was reduced at low luminance. In fact, when the retinal illuminance was reduced to 0.0785 scotopic td, which is below the human cone threshold of ~0.1 photopic td (Lee, Smith, Pokorny & Kremers, 1997), Takeuchi & De Valois (1997) found that ISIs no longer reversed perceived motion. We now show that the reversal of initial OFRs by ISIs was also much reduced under scotopic viewing conditions.

4.1. Methods

Many of the methods and procedures were identical to those used in Experiment 1, and only those that were different will be described here.

4.1.1. Subjects—Three subjects participated; two were authors (FAM, BMS) and the third was a paid volunteer who was unaware of the purpose of the experiments (JKM). All had normal or corrected-to-normal vision and viewing was always monocular (right eye viewing) with natural pupils.

4.1.2. Visual display and grating patterns—Motion stimuli again consisted of a two-image movie, this time using only pure sine-wave gratings with the same spatial frequency as the *1f* stimulus in Experiment 1, i.e., 0.153 cycles/° (wavelength, 6.55°).[3] The initial phase of the first image was randomized from trial to trial at intervals of ¼-wavelength, and the second image was identical to the first except phase shifted horizontally (rightward or leftward, randomly selected) by 1.65° (66 pixels), corresponding to ¼ of the wavelength of the fundamental of the *1f* stimulus. The ISIs were 0, 10, 20, 40, 60, 100, 140, and 200 ms, and the Michelson contrast was 32%. Each subject wore custom goggles that limited viewing to the right eye only (the recorded eye) and excluded all light sources other than the monitor screen displaying the grating stimuli. Neutral density filters were mounted in the goggles and the mean luminance of the display was adjusted so that the gratings had a mean retinal illuminance of 0.05 scotopic td, which is well below the human cone threshold of ~0.1 photopic td (Lee et al., 1997). For these estimates of the retinal illuminance, pupil diameters were measured (to the nearest 0.1 mm) from digital images obtained with flash photography after 25 min in complete darkness, which is the time it takes the pupil to reach its maximum steady-state size (Alpern & Ohba, 1972).[4]

4.1.3. Procedures—The search coil was inserted in the right eye, the custom goggles were fitted and the room was darkened. After performing the usual calibration procedure the subject sat facing the blank monitor screen (luminance <0.02 scotopic td) for a total of 25 min to dark adapt prior to the presentation of the OFR stimuli. The experiment then proceeded as in Experiments 1 and 2 except that the duration of the second of the two images was increased from 200 to 400 ms because the latency and duration of the initial OFRs were both much longer under scotopic conditions (see below).

4.2. Results

Figure 5A shows the mean R-L velocity response profiles obtained from one subject with ISIs ranging from 0–200 ms under scotopic conditions. The data are strikingly different from those previously seen in Fig. 1A, which showed the mean R-L velocity response profiles obtained from the same subject under photopic conditions with gratings of the same spatial frequency

---

[3]We used monocular viewing and gratings of low spatial frequency to reduce the likelihood that any shortcomings in vergence and accommodation under the scotopic viewing conditions—when foveal vision is compromised—would degrade the visual stimuli significantly.

[4]The steady-state size of the pupil is inversely related to the retinal illuminance, reaching maximum at ~0.1 scotopic td (Alpern & Ohba, 1972), hence we assume that the steady-state pupil size in complete darkness provides a good estimate of the steady-state pupil size in our experimental conditions (0.05 scotopic td).

("the *1f* stimulus") and contrast (32%), as well ISIs ranging over the same time period. Even the 0-ms ISI data were very different: compared with the 0-ms ISI data in Fig. 1A, those in Fig. 5a have an initial transient that has, *1)* an onset latency that is ~60 ms greater, *2)* a peak amplitude that is ~8-fold greater, *3)* a rise-time that is more than 100 ms longer, and *4)* a duration that is at least 8-fold greater. The 0-ms ISI data from the only other subject for whom we have data for comparable stimuli in the two luminance conditions (JKM) showed similar effects (not illustrated): under scotopic conditions the onset latency was ~100 ms longer, the peak amplitude was nearly 40-fold greater, and the rise-time was ~120 ms longer.[5] Thus, under scotopic conditions, the initial OFRs had much larger amplitudes and more sluggish dynamics than under photopic conditions. The effects of ISIs under scotopic conditions were also very different and this too is immediately apparent from a comparison of the mean R-L velocity response profiles in Figs. 5A and 1A: under photopic conditions an ISI of 10 ms was sufficient to reverse the initial OFR and the reversal reached a peak with an ISI of 40 ms, whereas under scotopic conditions an ISI of 10 ms merely resulted in a slight attenuation of the initial OFR, reversal did not occur until the ISI reached 60 ms and peak reversal did not occur until the ISI reached 100 ms. Furthermore, under photopic conditions the reversed OFR reached velocities that far exceeded (by ~140%) those achieved by the non-reversed OFR (with a 0-ms ISI), whereas under scotopic conditions the reversed OFR never reached velocities that were more than ~17% of those achieved by the non-reversed OFR (with a 0-ms ISI). The ISI data from the only other subject for whom we have data for comparable stimuli in the two situations (JKM) again showed similar effects (not illustrated): under photopic conditions the reversed OFR reached velocities that exceeded those achieved by the non-reversed OFR by >2000%, whereas under scotopic conditions the reversed OFR never reached velocities that were more than ~30% of those achieved by the non-reversed OFR (with a 0-ms ISI).

The dependence of the initial OFR on the ISI under scotopic conditions is also apparent from the (normalized) amplitudes of the mean R-L peak responses and their latencies, which are plotted in Figs. 5B and 5C, respectively, for all 3 subjects. It is now evident that, in all cases, the OFR was veridical with ISIs ≤40 ms and reversed with ISIs ≥60 ms, reaching a peak reversal with ISI of 60–100 ms and declining thereafter. The latency of the peak in the mean R-L velocity profile was always maximal with an ISI of 0 ms (range, 204–275 ms) and tended to decrease 30–50 ms as the ISI was increased, though there were major irregularities in this decline for 2 of the 3 subjects. The latency of the OFR onset showed little dependence on the ISI—see Fig. 5A, for example—so that most of these changes in the latency of the R-L peak in Fig. 5C reflected changes in the time-to-peak, i.e., the time from the onset of the response to the peak in the velocity profile.

4.3. Discussion of Experiment 3

The dependence of the initial OFR on the ISI was very sensitive to the mean luminance level: in Experiments 1 and 2, under photopic conditions, there was strong reversal of the initial OFR with ISIs of 10–60 ms, the reversed OFRs reaching much higher velocities than the non-reversed OFRs with 0-ms ISI, whereas in Experiment 3, under scotopic conditions, reversal occurred only with ISIs≥60 ms and then the reversed OFRs were always appreciably weaker than the non-reversed OFRs with 0-ms ISI. That the dependence of OFRs on the ISI shifted from biphasic to more monophasic with dark adaptation accords with the changes in the human modulation transfer function from band-pass to low-pass in the frequency domain and from biphasic to monophasic in the time domain (Kelly, 1961; 1971a; 1971b; Roufs, 1972a; 1972b; Snowden et al., 1995; Spekreijse et al., 1971; Swanson et al., 1987). Our findings are also reminiscent of those of Takeuchi & De Valois (1997), who also used 2-image movies with

---

[5]The initial OFR was less transient in this subject, the initial wave of eye velocity outlasting the open-loop period even under photopic conditions, precluding a comparison of the durations in the two conditions.

sinusoidal gratings and reported that ISIs of 30–90 ms resulted in clear reversal of perceived motion during photopic viewing but not during scotopic viewing. Although dark adaptation completely eliminated the reversal of perceived motion by ISIs in Takeuchi & De Valois's experiment it did not completely eliminate the reversal of the OFR by ISIs in our experiment, even though the retinal illuminance in our experiment (0.05 scotopic td) was slightly lower than in theirs (0.0785 scotopic td). This might in part reflect methodological differences in the two studies, particularly differences in the size and the spatial frequency of the grating patterns. Takeuchi & De Valois (1997) do not indicate the size of their display but, based on the size of their monitor ("16 in") and their viewing distance (115 cm), we estimate that it might have been as large as 20º (diagonally) and hence somewhat smaller than our display (which subtended 31.4º horizontally and 25.4º vertically). Takeuchi & De Valois's stimuli were also of higher spatial frequency than ours: 1 cycle/º vs 0.153 cycle/º. Both of these factors would be expected to render Takeuchi & De Valois's data more low-pass—and hence more monophasic—than ours (Snowden et al., 1995; Swanson et al., 1987; Takeuchi & De Valois, 2000). It is also possible that our methodology—based on high-resolution eye-movement recordings—is better able to resolve the smaller signals at low luminance levels.

The initial OFRs elicited by two-image movies without an ISI were also very sensitive to the mean luminance level and had appreciably larger amplitudes as well as much more sluggish dynamics—including longer latency, time-to-peak and duration—in the scotopic conditions of Experiment 3 than in the photopic conditions of Experiment 1. (Note that, in contrast, the maximum eye velocities achieved during the ISI-induced reversals of the OFRs were quite similar in scotopic and photopic conditions.) Apropos the increased OFR amplitudes at low luminance, we have been unable to find any previous studies that reported increases in human contrast sensitivity with dark adaptation, the usual finding being little or no change at low spatial and temporal frequencies (approximating Weber's Law) and decreases at higher frequencies (De Valois, Morgan & Snodderly, 1974; Kelly, 1961; Snowden et al., 1995; Spekreijse et al., 1971; Swanson et al., 1987). One might expect that the initial OFR to a 2-image movie—a velocity-impulse stimulus—would be very sensitive to any changes in the amplitude of the temporal impulse response of the human visual system but the latter is known to decrease substantially with dark adaptation (Swanson et al., 1987). The sluggish dynamics of the initial OFR at low luminance was not unexpected because, as mentioned in the previous paragraph, the human modulation transfer function shifts from band-pass to low-pass with dark adaptation, and both the time-to-peak and the duration of the associated temporal impulse responses show increases with dark adaptation (see Fig. 3 in Swanson et al., 1987). However, these increases are less than half those that we are reporting for the initial transient OFR. Of course, the increased amplitude of the initial transient OFR at low luminance is in part linked to its increased duration but might also be in part secondary to its increased latency: the latter means that the system has more time to integrate the motion-error signal before responding, a factor that has been invoked in the past to explain anomalous increases in the amplitude of the monkey's initial OFR with decreases in contrast (Miles et al., 1986). Some, if not all, of the increase in the latency of OFRs with dark adaptation might be accounted for by the longer latency of rod responses relative to cone responses (Lee et al., 1997).

Data from lesions and neurophysiology in monkeys strongly implicate the cortical area MST in the genesis of the earliest OFR (Kawano, Inoue, Takemura, Kodaka & Miles, 2000; Kawano, Shidara, Watanabe & Yamane, 1994; Miles, 1998; Takemura, Inoue & Kawano, 2002). This cortical region is specialized for motion processing (for recent review, see Wurtz, 1998) and is thought to rely heavily on magnocellular pathways, which are so named because they include the magnocellular layers of the LGN (Livingstone & Hubel, 1988; Livingstone & Hubel, 1987; Maunsell, Nealey & DePriest, 1990; Merigan & Maunsell, 1990; Schiller, Logothetis & Charles, 1990). The contrast-dependence of the OFR in monkeys (Miles et al., 1986) and humans (Masson & Castet, 2002; Sheliga et al., 2005) closely resembles that in the

magnocellular pathway, which is characterized by saturation at relatively low contrast levels (Kaplan & Shapley, 1982). Recordings from monkeys indicate that, at scotopic luminance levels, vision is dominated by rod inputs to magnocellular-projecting retinal ganglion cells (Lee et al., 1997; Purpura, Kaplan & Shapley, 1988), consistent with our finding that the OFR continues to operate even at very low luminance and contrast levels.

4. Closing Remarks

In a previous study we used the missing fundamental stimulus to initiate OFRs and showed that the Fourier composition of the spatial stimulus was a critical determinant of the responses, indicating that the underlying detectors do not sense the motion of the raw images (or their features) but rather a spatially filtered version of the images. The present paper has used an ISI to show that the temporal characteristics of that stimulus are also critical and uncovered some important dynamical features of the visual input reaching the motion detectors. Thus, although the initial OFR is a motor response, it directly reflects the spatio-temporal properties of the early visual pathways that are important for motion processing. With clear evidence that the OFR uses 1st-order motion sensing mechanisms and is mediated by magnocellular inputs to cortical area MST, we suggest that the initial OFR provides a model system for objective, quantitative studies of the early cortical processing of visual motion.

References

Adelson EH. Some new motion illusions, and some old ones, analysed in terms of their Fourier components. Investigative Ophthalmology and Visual Science 1982;34(Suppl):144.Abstract

Adelson EH, Bergen JR. Spatiotemporal energy models for the perception of motion. Journal of the Optical Society of America A 1985;2:284–299.

Alpern M, Ohba N. The effect of bleaching and backgrounds on pupil size. Vision Research 1972;12:943–951. [PubMed: 5037710]

Baro JA, Levinson E. Apparent motion can be perceived between patterns with dissimilar spatial frequencies. Vision Research 1988;28:1311–1313. [PubMed: 3256148]

Bergen JR, Wilson HR. Prediction of flicker sensitivities from temporal three-pulse data. Vision Research 1985;25:577–582. [PubMed: 4060611]

Bex PJ, Baker CL Jr. Motion perception over long interstimulus intervals. Perception & Psychophysics 1999;61:1066–1074. [PubMed: 10497428]

Boulton JC, Baker CL Jr. Dependence on stimulus onset asynchrony in apparent motion: evidence for two mechanisms. Vision Research 1993;33:2013–2019. [PubMed: 8249316]

Braddick OJ. Low-level and high-level processes in apparent motion. Philosophical Transactions of the Royal Society B Biological Sciences 1980;290:137–151.

Brainard DH. The Psychophysics Toolbox. Spatial Vision 1997;10:433–436. [PubMed: 9176952]

Brown RO, He S. Visual motion of missing-fundamental patterns: motion energy versus feature correspondence. Vision Research 2000;40:2135–2147. [PubMed: 10878275]

Burr DC, Morrone MC. Temporal impulse response functions for luminance and colour during saccades. Vision Research 1996;36:2069–2078. [PubMed: 8776473]

Chen KJ, Sheliga BM, Fitzgibbon EJ, Miles FA. Initial ocular following in humans depends critically on the fourier components of the motion stimulus. Annals of the New York Academy of Sciences 2005;1039:260–271. [PubMed: 15826980]

Collewijn H, Van Der Mark F, Jansen TC. Precise recording of human eye movements. Vision Research 1975;15:447–450. [PubMed: 1136166]

De Valois RL, Morgan H, Snodderly DM. Psychophysical studies of monkey vision. III. Spatial luminance contrast sensitivity tests of macaque and human observers. Vision Research 1974;14:75–81. [PubMed: 4204839]

Derrington AM, Allen HA, Delicato LS. Visual mechanisms of motion analysis and motion perception. Annual Review of Psychology 2004;55:181–205.

Gellman RS, Carl JR, Miles FA. Short latency ocular-following responses in man. Visual Neuroscience 1990;5:107–122. [PubMed: 2278939]

Georgeson MA, Harris MG. The temporal range of motion sensing and motion perception. Vision Research 1990;30:615–619. [PubMed: 2339514]

Georgeson MA, Shackleton TM. Monocular motion sensing, binocular motion perception. Vision Research 1989;29:1511–1523. [PubMed: 2635477]

Hammett ST, Ledgeway T, Smith AT. Transparent motion from feature- and luminance-based processes. Vision Research 1993;33:1119–1122. [PubMed: 8506650]

Hays AV, Richmond BJ, Optican LM. A UNIX-based multiple process system for real-time data acquisition and control. WESCON Conference Proceedings 1982;2:1–10.

Ikeda M. Temporal summation of positive and negative flashes in the visual system. Journal of the Optical Society of America 1965;55:1527–1534.

Ikeda M. Temporal impulse response. Vision Research 1986;26:1431–1440. [PubMed: 3303667]

Kaplan E, Shapley RM. X and Y cells in the lateral geniculate nucleus of macaque monkeys. Journal of Physiology 1982;330:125–143. [PubMed: 7175738]

Kawano K, Inoue Y, Takemura A, Kodaka Y, Miles FA. The role of MST neurons during ocular tracking in 3D space. International Review of Neurobiology 2000;44:49–63. [PubMed: 10605641]

Kawano K, Shidara M, Watanabe Y, Yamane S. Neural activity in cortical area MST of alert monkey during ocular following responses. Journal of Neurophysiology 1994;71:2305–2324. [PubMed: 7931519]

Kelly DH. Visual response to time-dependent stimuli. I. Amplitude sensitivity measurements. Journal of the Optical Society of America 1961;51:422–429. [PubMed: 13752375]

Kelly DH. Theory of flicker and transient responses. I. Uniform fields. Journal of the Optical Society of America 1971a;61:537–546. [PubMed: 4323022]

Kelly DH. Theory of flicker and transient responses. II. Counterphase gratings. Journal of the Optical Society of America 1971b;61:632–640. [PubMed: 4323629]

Lee BB, Smith VC, Pokorny J, Kremers J. Rod inputs to macaque ganglion cells. Vision Research 1997;37:2813–2828. [PubMed: 9415362]

Livingstone M, Hubel D. Segregation of form, color, movement, and depth: anatomy, physiology, and perception. Science 1988;240:740–749. [PubMed: 3283936]

Livingstone MS, Hubel DH. Psychophysical evidence for separate channels for the perception of form, color, movement, and depth. The Journal of Neuroscience 1987;7:3416–3468. [PubMed: 3316524]

Lu ZL, Sperling G. The functional architecture of human visual motion perception. Vision Research 1995;35:2697–2722. [PubMed: 7483311]

Lu ZL, Sperling G. Three-systems theory of human visual motion perception: review and update. Journal of the Optical Society of America A 2001;18:2331–2370.

Masson GS, Busettini C, Yang DS, Miles FA. Short-latency ocular following in humans: sensitivity to binocular disparity. Vision Research 2001;41:3371–3387. [PubMed: 11718780]

Masson GS, Castet E. Parallel motion processing for the initiation of short-latency ocular following in humans. The Journal of Neuroscience 2002;22:5149–5163. [PubMed: 12077210]

Masson GS, Yang DS, Miles FA. Reversed short-latency ocular following. Vision Research 2002a;42:2081–2087. [PubMed: 12169427]

Masson GS, Yang DS, Miles FA. Version and vergence eye movements in humans: open-loop dynamics determined by monocular rather than binocular image speed. Vision Research 2002b;42:2853–2867. [PubMed: 12450510]

Maunsell JH, Nealey TA, DePriest DD. Magnocellular and parvocellular contributions to responses in the middle temporal visual area (MT) of the macaque monkey. The Journal of Neuroscience 1990;10:3323–3334. [PubMed: 2213142]

Merigan WH, Maunsell JH. Macaque vision after magnocellular lateral geniculate lesions. Visual Neuroscience 1990;5:347–352. [PubMed: 2265149]

Miles FA. The neural processing of 3-D visual information: evidence from eye movements. The European Journal of Neuroscience 1998;10:811–822. [PubMed: 9753150]

Miles FA, Kawano K, Optican LM. Short-latency ocular following responses of monkey. I. Dependence on temporospatial properties of visual input. Journal of Neurophysiology 1986;56:1321–1354. [PubMed: 3794772]

Naka KI, Rushton WA. S-potentials from colour units in the retina of fish (Cyprinidae). Journal of Physiology 1966;185:536–555. [PubMed: 5918058]

Nishida S. Spatiotemporal properties of motion perception for random-check contrast modulations. Vision Research 1993;33:633–645. [PubMed: 8351836]

Pantle A, Turano K. Visual resolution of motion ambiguity with periodic luminance- and contrast-domain stimuli. Vision Research 1992;32:2093–2106. [PubMed: 1304087]

Pelli DG. The VideoToolbox software for visual psychophysics: transforming numbers into movies. Spatial Vision 1997;10:437–442. [PubMed: 9176953]

Pelli DG, Zhang L. Accurate control of contrast on microcomputer displays. Vision Research 1991;31:1337–1350. [PubMed: 1891822]

Purpura K, Kaplan E, Shapley RM. Background light and the contrast gain of primate P and M retinal ganglion cells. Proceedings of the National Academy of Sciences 1988;85:4534–4537.

Rashbass C. The visibility of transient changes of luminance. Journal of Physiology 1970;210:165–186. [PubMed: 5500775]

Robinson DA. A method of measuring eye movement using a scleral search coil in a magnetic field. Institute of Electronic and Electrical Engineers: Transactions in Biomedical Engineering, BME 1963;10:137–145.

Roufs JAJ. Dynamic properties of vision. I. Experimental relationships between flicker and flash thresholds. Vision Research 1972a;12:261–278. [PubMed: 5033689]

Roufs JAJ. Dynamic properties of vision. II. Theoretical relationships between flicker and flash thresholds. Vision Research 1972b;12:279–292. [PubMed: 5033690]

Schiller PH, Logothetis NK, Charles ER. Role of the color-opponent and broad-band channels in vision. Visual Neuroscience 1990;5:321–346. [PubMed: 2265148]

Sheliga BM, Chen KJ, FitzGibbon EJ, Miles FA. Initial ocular following in humans: a response to first-order motion energy. Vision Research 2005;45:3307–3321. [PubMed: 15894346]

Shioiri S, Cavanagh P. ISI produces reverse apparent motion. Vision Research 1990;30:757–768. [PubMed: 2378068]

Smith AT. Correspondence-based and energy-based detection of second-order motion in human vision. Journal of the Optical Society of America A 1994;11:1940–1948.

Smith AT, Hess RF, Baker CL Jr. Direction identification thresholds for second-order motion in central and peripheral vision. Journal of the Optical Society of America A - Optics and Image Science 1994;11:506–514.

Snowden RJ, Hess RF, Waugh SJ. The processing of temporal modulation at different levels of retinal illuminance. Vision Research 1995;35:775–789. [PubMed: 7740769]

Solomon JA, Sperling G. Full-wave and half-wave rectification in second-order motion perception. Vision Research 1994;34:2239–2257. [PubMed: 7941419]

Spekreijse H, van Norren D, van den Berg TJ. Flicker responses in monkey lateral geniculate nucleus and human perception of flicker. Proceedings of the National Academy of Sciences 1971;68:2802–2805.

Strout JJ, Pantle A, Mills SL. An energy model of interframe interval effects in single-step apparent motion. Vision Research 1994;34:3223–3240. [PubMed: 7975353]

Swanson WH, Ueno T, Smith VC, Pokorny J. Temporal modulation sensitivity and pulse-detection thresholds for chromatic and luminance perturbations. Journal of the Optical Society of America A 1987;4:1992–2005.

Takemura A, Inoue Y, Kawano K. Visually driven eye movements elicited at ultra-short latency are severely impaired by MST lesions. Annals of the New York Academy of Sciences 2002;956:456–459. [PubMed: 11960839]

Takeuchi T, De Valois KK. Motion-reversal reveals two motion mechanisms functioning in scotopic vision. Vision Research 1997;37:745–755. [PubMed: 9156219]

Takeuchi T, De Valois KK. Velocity discrimination in scotopic vision. Vision Research 2000;40:2011–2024. [PubMed: 10828468]

Takeuchi T, De Valois KK, Motoyoshi I. Light adaptation in motion direction judgments. Journal of the Optical Society of America A 2001;18:755–764.

Tong J, Peng P, Sun F. Alternating optokinetic nystagmus (OKN) induced by intermittent display of stationary gratings. Experimental Brain Research 2003;148:545–548.

Tong J, Wang J, Sun F. Dual-directional optokinetic nystagmus elicited by the intermittent display of gratings in primary open-angle glaucoma and normal eyes. Current Eye Research 2002;25:355–362. [PubMed: 12789542]

van Santen JP, Sperling G. Elaborated Reichardt detectors. Journal of the Optical Society of America A 1985;2:300–321.

Watson AB, Ahumada AJ Jr. Model of human visual-motion sensing. Journal of the Optical Society of America A - Optics and Image Science 1985;2:322–341.

Wurtz RH. Optic flow: A brain region devoted to optic flow analysis? Current Biology 1998;8:R554–556. [PubMed: 9707391]

Yang DS, FitzGibbon EJ, Miles FA. Short-latency disparity-vergence eye movements in humans: sensitivity to simulated orthogonal tropias. Vision Research 2003;43:431–443. [PubMed: 12536000]

Yang DS, Miles FA. Short-latency ocular following in humans is dependent on absolute (rather than relative) binocular disparity. Vision Research 2003;43:1387–1396. [PubMed: 12742108]
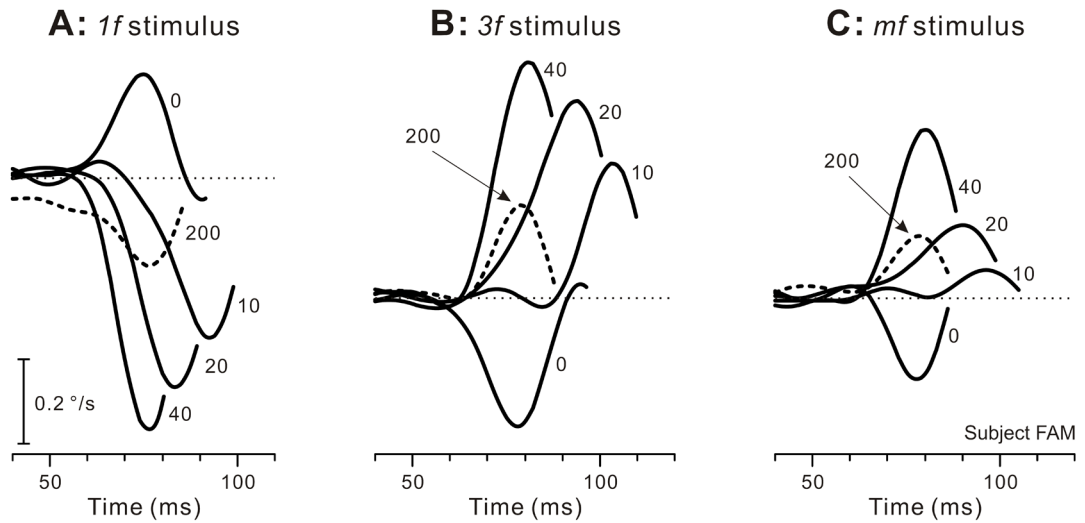
A: *1f* stimulus

B: *3f* stimulus

C: *mf* stimulus

Fig. 1.
The initial horizontal OFRs elicited by two-image movies applied to various vertical gratings: dependence of mean R-L velocity response profiles on an intervening luminance-matched period of gray, the ISI (subject, FAM). A: A sinusoidal grating of wavelength 6.55°, the *1f* stimulus. B: A sinusoidal grating of wavelength 2.183°, the *3f* stimulus. C: A square-wave grating of wavelength 6.55° with a missing fundamental, the *mf* stimulus. The phase differences between the two frames of the movies resulted in 1.65° steps corresponding to ¼ of the wavelength of the fundamental of the *1f* and *mf* stimuli and ¾ of the wavelength of the *3f* stimulus. Each trace is the mean response to 181–241 repetitions of the stimulus. Note that time on the abscissa starts 40 ms after the appearance of the 2nd image. The numbers on the traces indicate the ISIs in ms. Upward deflections of the traces denote forward eye movements in the direction of the steps, the dotted lines indicating zero eye velocity. Contrast was 32% for the pure sinusoids and for the *3f* component of the *mf* stimulus.
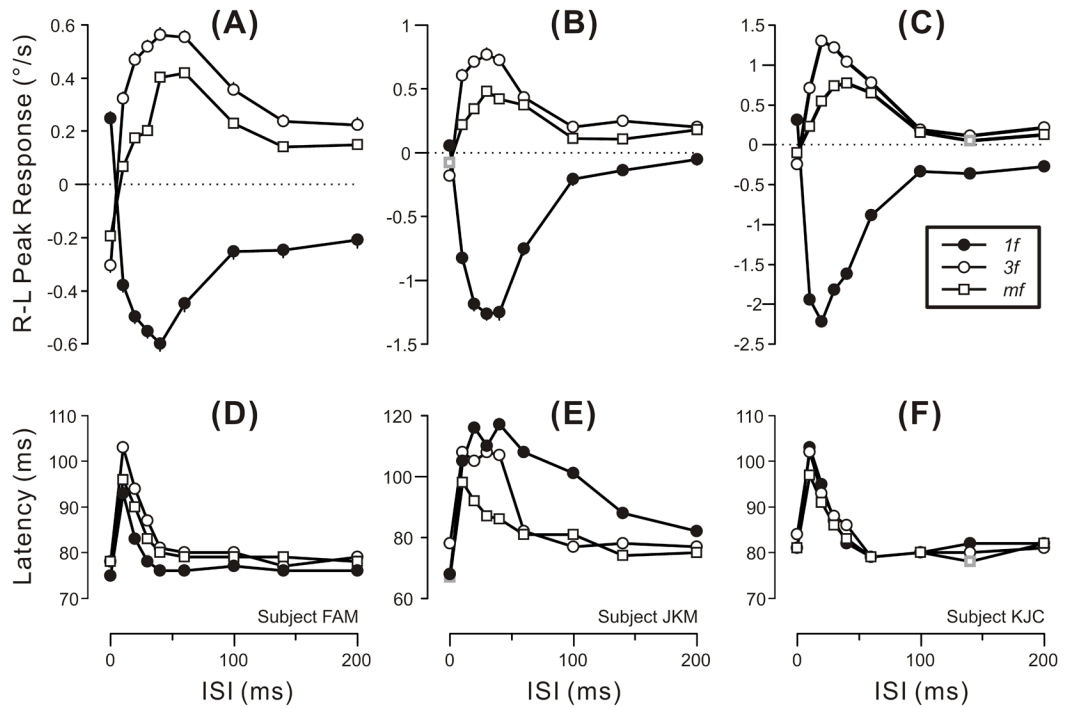
Fig. 2.
The initial horizontal OFRs elicited by two-image movies applied to various vertical gratings: dependence of mean R-L peak velocity (upper plots) and latency of the R-L peaks (lower plots) on the ISI (mean data for each of 3 subjects). Positive peak responses denote forward tracking, i.e., in the direction of the applied 1.65° steps (error bars, SE's). Peak latencies were measured from the appearance of the 2nd frame using the mean R-L eye velocity traces (so there are no error bars). Filled circles: *1f* stimulus. Open circles: *3f* stimulus. Open squares: *mf* stimulus. Gray symbols: the 2/81 peak responses that failed to exceed 3 SDs and so were selected by hand. A,D: subject FAM (181–241 trials per condition; SDs ranged from 0.35–0.43°/s). B,E: subject JKM (167–223 trials per condition; SDs ranged from 0.48–0.80°/s). C,F: subject KJC (189–250 trials per condition; SDs ranged from 0.45–0.78°/s). Error bars, SE's. Contrast was 32% for the pure sinusoids and for the *3f* components of the *mf* stimulus.
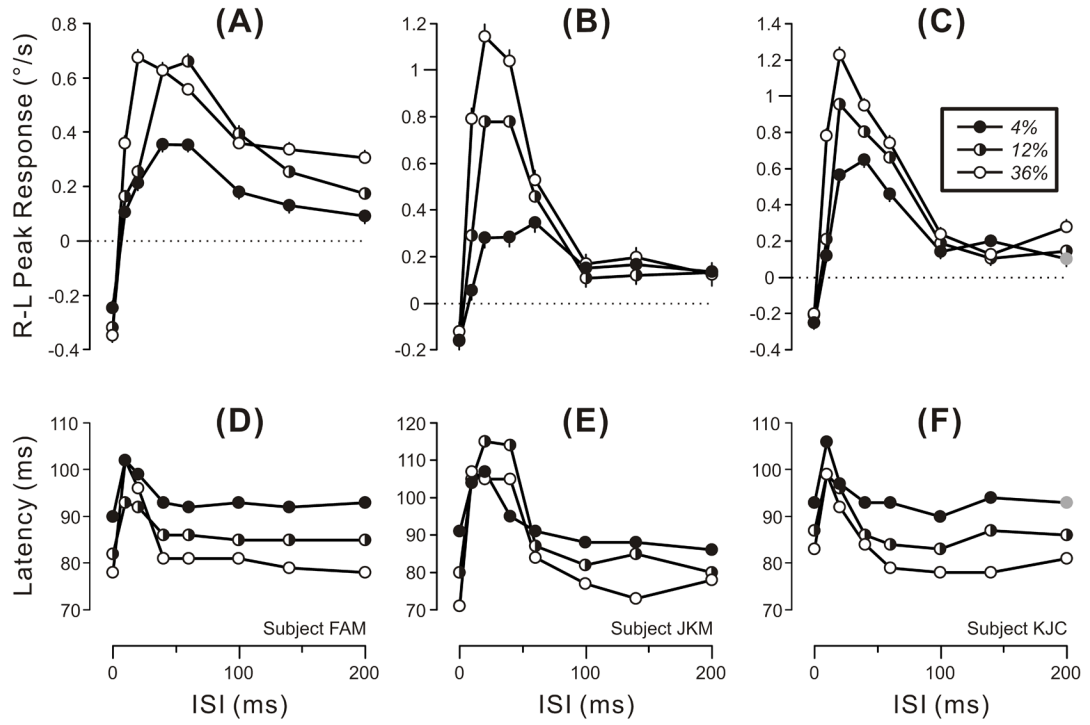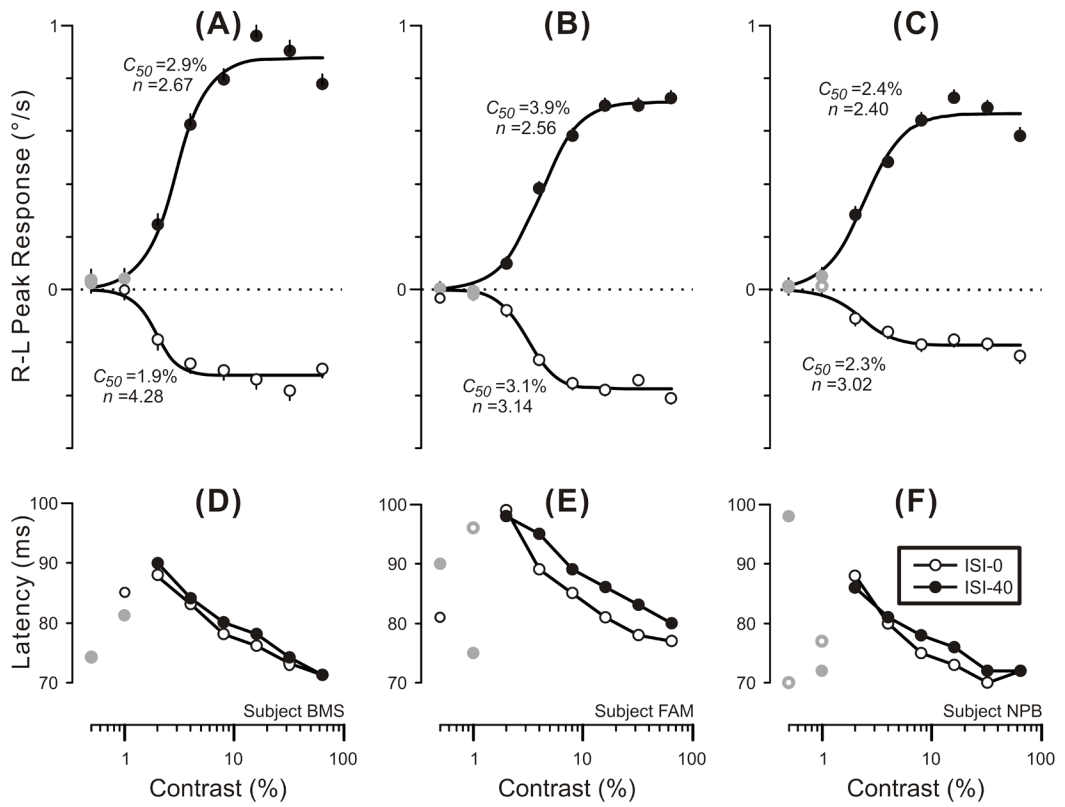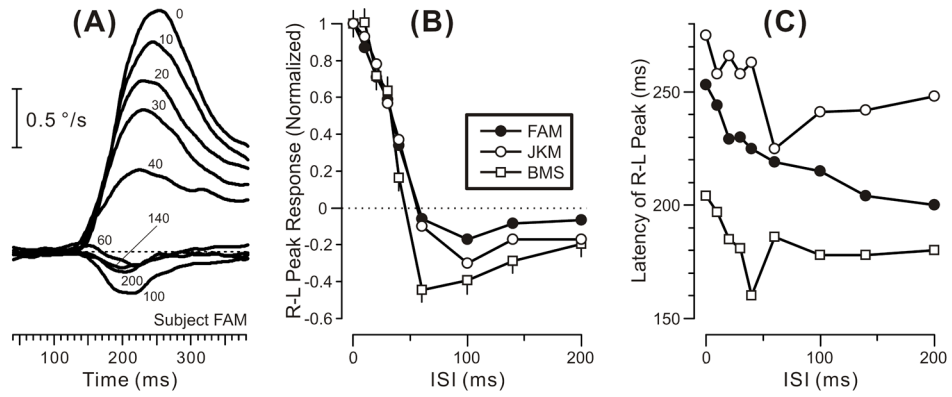
Fig. 3.
The initial horizontal OFRs elicited by two-image movies applied to vertical *3f* gratings of various contrasts: dependence of mean R-L peak velocity (upper plots) and latency of the R-L peak (lower plots) on the ISI (data for each of 3 subjects). Positive peak responses denote tracking in the direction of the applied 1.65° steps (error bars, SEs). Peak latencies were measured from the appearance of the 2nd frame using the mean R-L eye velocity traces (so there are no error bars). Filled circles: 4% contrast. Half-filled circles: 12% contrast. Open circles: 36% contrast. Gray symbols: 1/72 responses that failed to exceed 3 SDs and so was selected by hand. A,D: subject FAM (191–234 trials per condition; SDs ranged from 0.36–0.45°/s). B,E: subject JKM (179–245 trials per condition; SDs ranged from 0.54–0.84°/s). C,F: subject KJC (193–243 trials per condition; SDs ranged from 0.49–0.68°/s). Error bars, SE's.

Fig. 4.
The initial horizontal OFRs elicited by two-image movies applied to vertical *3f* gratings with an ISI of 0 ms or 40 ms: dependence of mean R-L peak velocity (upper plots) and latency of the R-L peak (lower plots) on contrast (data for each of 3 subjects). Positive peak responses denote tracking in the direction of the applied 1.65° steps and the smooth black curves are best-fit Naka-Rushton functions (Expression 1) with the values of their c_{50} and n parameters shown nearby (error bars, SEs). Peak latencies were measured from the appearance of the 2nd frame using the mean R-L eye velocity traces (so there are no error bars). Open circles: 0-ms ISI. Closed circles: 40–ms ISI. Gray symbols: 10/48 responses that failed to exceed 3 SDs and were selected by hand. A,D: subject BMS (143–154 trials per condition; SDs ranged from 0.42–0.50°/s). B,E: subject FAM (282–303 trials per condition; SDs ranged from 0.37–0.45°/s). C,F: subject NPB (189–201 trials per condition; SDs ranged from 0.37–0.43°/s). Error bars, SE's.

Fig. 5.
The initial horizontal OFRs elicited by two-image movies applied to vertical *1f* gratings under scotopic conditions: dependence on the ISI. A: Sample mean R-L eye velocity profiles for one subject (FAM); positive responses denote tracking in the direction of the applied 1.65° steps and the numbers on the traces indicate the ISI in ms; note that time on the abscissa starts 40 ms after the appearance of the 2nd image. B: Dependence of mean R-L peak responses on ISI for all 3 subjects, each normalized with respect to their responses with 0-ms ISI (error bars, SEs). C: Dependence of R-L peak latencies on ISI for all 3 subjects. Open squares: subject BMS (213-288 trials per condition; SDs ranged from 1.02–1.23). Filled circles: subject FAM (314–348 trials per condition; SDs ranged from 0.29–0.46). Open circles: subject JKM (177–200 trials per condition; SDs ranged from 0.35–0.47). Viewing monocular. Contrast, 32%.